# Contribution of Arc Plasma Radiation Energy to Electrodes†

Masao USHIO*, Ding FAN** and Manabu TANAKA***

**Abstract**

*Recent investigation shows that the interplay between an arc and electrodes is much more complex than what has been understood. In order to make a further understanding of the energy balance in the electrodes of a thermal arc plasma, we have proposed a simple model for estimating the cathode fall voltage. This paper analyzes the contribution of arc radiation to the rod cathode and anode plate based on the mathematic model of arc heat transfer and the previously experimental relation of arc radiation coefficient versus arc temperature. The results show that contribution of arc radiation energy to the electrodes is small as compared to the electron cooling energy in cathode or heating energy in anode plate with arc current from 100A to 300A. The arc radiation energy, to some extent, may have effects in some case, but dose not play a dominant role in the cathode or anode energy balance.*

**KEY WORDS:** (Thermal Plasma) (GTA) (Arc Radiation) (Radiation Coefficient) (Cathode Energy Balance)

## 1. Introduction

With the increasing application of thermal plasma in today's industries such as welding, spraying, cutting, surface modification, metal refining and dust treatment etc., investigation of the interaction between an arc and the electrode materials is more interest. Heat transfer is one of the main processes. In high current gas-tungsten-arc discharge, for example, the erosion of cathode materials is a serious problem, which is mainly controlled by the energy balance in the cathode surface[1,2]. Although many efforts have been devoted to the research of cathode energy balance[2,3], unfortunately, so far it is still unclear problem. Most of the researchers neglected the contribution of arc radiation energy to the electrodes. However, recently some one[4] suggested the arc radiation energy plays a dominant role in the cathode energy balance[3].

On the other hand, it is well known that in an arc discharge the electron energy, due to the work function of anode material and anode fall voltage, occupies a dominant part of the energy input to the anode[5-8]. Recently, however some researchers have found the arc anode fall voltage is minus[9].

All this shows the interplay between the arc plasma and electrodes is much more complex than what has been understood and it is worth to make deeper investigations. In order to make a further understanding of the energy balance in the electrodes of an arc plasma, we have proposed a simple model for estimating the cathode fall voltage of thermal atmospheric arcs[10]. In this paper, the contributions of arc radiation to the electrodes are numerically analyzed based on the mathematic model of the arc heat transfer[11] and the experimental relation between the arc plasma radiation coefficient and arc temperatures by Evans and Tankin et al.[12-14]. And the relative effect of arc radiation energy on the electrode energy balance is discussed.

## 2. Computing Approach

### 2.1 Formulation

The axis-symmetric coordinate system and the spatial geometric relations among various variables used in the following are schematically shown in **Fig.1.** Let us consider a volume element of the arc plasma $dv$, at a spatial point $A$ $(r, \beta, z)$, uniformly emits energy to the space, then the energy density received and absorbed by

† Received on Dec. 20, 1993
* Professor
** Graduate Student
*** Research Associate

Transactions of JWRI is published by Welding Research Institute, Osaka University, Ibaraki, Osaka 567, Japan

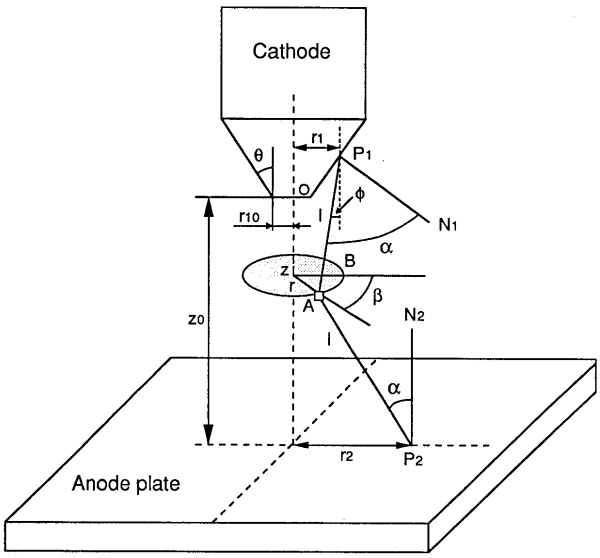


**Fig.1** Schematic diagram of coordinate system and relations of variables.

the anode plate at a point $P_2$ in a distance $r_2$ from the axis can be expressed as

$$dR_a(r_2) = \frac{\varepsilon_a U(r,z)}{4\pi l^2} \cos\alpha \, dv \quad (1)$$

$$l^2 = z'^2 + r^2 + r_2^2 - 2r\, r_2 \cos\beta, \quad z' = z_0 - z \quad (2)$$

$$\cos\alpha = \frac{z'}{l} \quad (3)$$

where

$U(r, z)$ : Plasma radiation power per unit volume ($W/m^3$) at point $A$ $(r, z)$

$\varepsilon_a$ : Absorptivity of the anode plate

$\alpha$ : Angle between the incident light and the surface normal direction at $P_2$ or $P_1$

$z_0$ : Arc length

$\theta$ : Half angle of electrode tip

$\phi$ : Angle between the incident light and $z$ axis at point $P_1$

$r_{10}$ : Radius of flat arc spot

$l$ : Distance from emitting point $A$ to target point $P_2$ or $P_1$

The total radiation energy absorbed by per unit area of anode surface at point $P_2$ can be obtained through integrating Eq.1 in the whole arc plasma volume shown as Eq.4.

$$R_a(r_2) = \int_V \frac{\varepsilon_a U(r,z)}{4\pi l^2} \cos\alpha \, dv = \int_0^{z_0}\int_0^{R_\infty}\int_0^{2\pi} \frac{\varepsilon_a U(r,z)(z_0 - z) r\, d\beta\, dr\, dz}{4\pi\left((z_0 - z)^2 + r^2 + r_2^2 - 2r r_2 \cos\beta\right)^{3/2}} \quad (4)$$

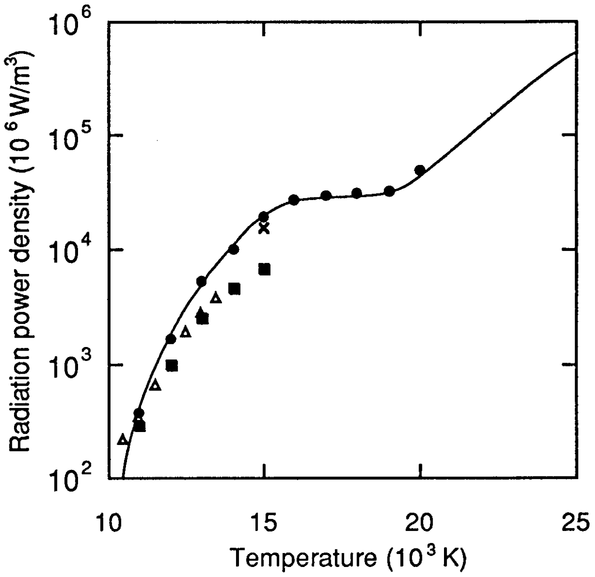


**Fig.2** Radiation power density of argon arc plasma at 1atm., compiled from (●) Evans and Tankin, (△) Emmons, (■) Bues et al. and (×) Olsen. Solid curve represents actual values of arc radiation power density used in the calculation[14].

where $R_\infty$ : Arc boundary

For a cathode electrode with a flat tip, the formula for calculating the radiation energy density is similar to Eq.4 and expressed as Eq.5.

$$R_{c1}(r_1) = \int_0^{z_0}\int_0^{R_\infty}\int_0^{2\pi} \frac{\varepsilon_c U(r,z)\, z\, r\, d\beta\, dr\, dz}{4\pi\left(z^2 + r^2 + r_1^2 - 2r r_1 \cos\beta\right)^{3/2}} \quad (5)$$

where $\varepsilon_c$ : Absorptivity of cathode material

If the cathode tip, or a part of it, is a cone, then as shown in Fig.1, a part of the plasma can not emit energy to some parts of the cathode surface where it can not be seen by the emitting site. And the condition is given by Eq.6.

$$\alpha \geq 90^\circ, \quad \alpha = \phi + (90^\circ - \theta) = 90^\circ + (\phi - \theta) \quad (6)$$

Thus the formula for calculating the radiation energy density of the conic surface can be expressed by Eq.7 ~ Eq.10.

$$\cos\alpha = \cos(90^\circ - \theta)\cos\phi - \sin(90^\circ - \theta)\sin\phi \quad (7)$$

$$\cos\phi = \frac{z'}{l}, \quad z' = z + \frac{(r_1 - r_{10})}{\tan\theta} \quad (8)$$

$$l^2 = z'^2 + r^2 + r_1^2 - 2r\, r_1 \cos\beta \quad (9)$$

$$R_{c2}(r_1) = \iiint_V \frac{\varepsilon_c U(r,z)\cos\alpha \; r\, d\beta\, dr\, dz}{4\pi l^2} \quad (10)$$

The integral limit is $\alpha \leq 90^\circ$ or $\phi \leq \theta$

## 2.2 Radiation power density of the argon plasma

The radiation of a plasma has two different types. When excited neutral atoms or ions return to the ground state in one or several steps, the emitted radiation appears as spectral lines, namely," the line radiation". The line emission coefficient is decided by all the possible transition probability (bound-bound) and particles density in the state. Another is the "continuum radiation" which is caused by the Bremsstrahlung effect (free-free transition) due to free electrons in plasma losing kinetic energy in the Coulomb field of positive ions, and to some extent also may be produced by the recombination of electrons with positive ions. The emission coefficient of the continuum radiation is dominantly decided by the plasma temperature and the electron and ion density. After all, the total radiation power density of an arc plasma is a function of the plasma temperature and pressure when the magnetic field is small.

An exact theoretical calculation of the total radiation coefficient of a plasma over the entire wavelength range is still difficult except hydrogen[15], though Cram has presented a method of statistical evaluation of the line radiation power loss from the argon thermal plasma with iron vapor[16]. Experimental study of argon plasma radiation have been carried out by Evans and Tankin[12], Emmans[13], and others. **Figure 2** shows the measured net radiation coefficient of argon arc plasma as a function of temperature at 1atm, which was compiled by Kovitya et al.[14]. The solid curve represents actual values used in the calculations and the unit is carefully changed to Joule per unit volume and time (W/m$^3$), i.e., the energy power density.

## 2.3 Arc temperature distribution

The arc temperature has been measured by a number of researchers such as Olsen(1957), Gick(1973), Seeger and Tiller(1979), Kobayashi and Suga(1979), Key et al.(1983), Haddad and Farmer(1985) [17-24]. As summarized by Lancaster[3] that because of different measuring methods the measured temperature distribution of GTA has two groups, namely, the higher peak temperature (about 20000K) and the lower peak temperature (10000K). On the other hand, recently, numerical computation by means of MHD mathematic models have made much achievements such as Ushio and Matsuda(1982), Hsu and Pfender(1983), Kovitya and Lowke(1985), Choo and Szekely(1990) [11,25,14,26]. The numerical results are found to agree well with the experimental results of higher peak temperature group which is confirmed by many of resent experiments. In this study, the mathematic model [11] which takes the

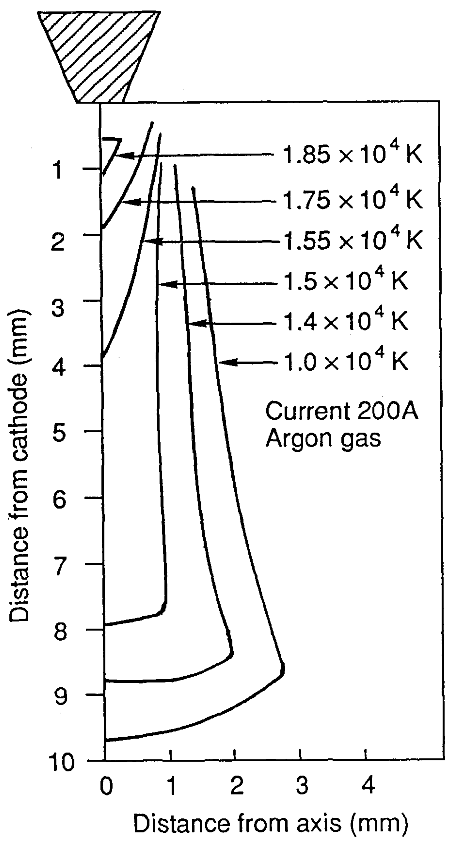


**Fig.3** Computed temperature contours of a 200A arc.

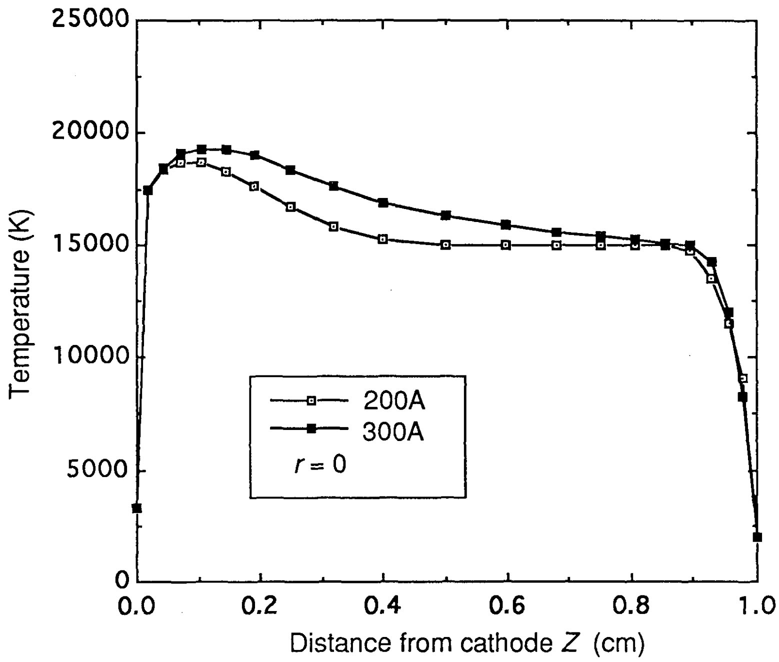


**Fig.4** Computed arc temperature distributions along the z axis.

turbulent flow into account is applied to calculate the arc temperature distribution, while instead of presetting the arc current distribution in the original model, the Ohm's law and charge continuity equation are introduced into the governing equations for determining the spatial distribution of current density in the study. The main equations are shown as following.

The mass conservation equation :

$$\rho\nabla\cdot\mathbf{U}=0 \tag{11}$$

The momentum conservation equation :

$$(\rho\mathbf{U}\cdot\nabla)\mathbf{U}=-\nabla P+\nabla\tau+\mathbf{F} \tag{12}$$

The energy conservation equation :

$$\rho\mathbf{U}\cdot\nabla h=\nabla(\lambda_{ef}\nabla T)+\mathbf{J}\cdot\mathbf{E}-S_r \tag{13}$$

The Ohm's law and current density conservation equation:

$$\mathbf{J}=\sigma\mathbf{E},\quad \nabla\cdot\mathbf{J}=0 \tag{14}$$

where

$\mathbf{U}$ : velocity vector, $\rho$ : mass density,
$P$ : pressure, $\tau$ : stress tensor,
$\mathbf{F}$ : electromagnetic force vector,
$\lambda_{ef}$ : effective thermal conductivity,
$\mathbf{J}$ : current density vector,
$S_r$ : radiation loss, $h$ : enthalpy,
$T$ : temperature

For the boundary conditions Ref.11 is referenced.

### 2.4. Solving procedure

The equations concerned with arc temperature (Eq.11~14) are numerically solved by means of FDM. Sequentially, the calculated temperature is applied to determine the radiation power density of the arc plasma according to Fig.2. And then Eq.4, 5 or 10 are numerically integrated in the whole arc plasma to obtain the distribution of absorbed radiation energy density on the cathode electrode and anode plate. The total radiation energy is easily achieved by integrating the energy density on the concerned surfaces. All the computations are carried out under the conditions of a free burning GTA plasma, Th-W electrode 3.2mm in diameter, 100 ~ 300A in arc current and 10mm in arc length, with argon and at atmospheric pressure. The calculated typical temperature distributions are shown in **Fig.3**, **Fig.4** and **Fig.5**. Obviously, these results are in accordance with the measurements of higher peak temperature group. The highest temperature and high temperature profile are a little lower compared to the results of Ref.14 and 25. This is because the turbulent flow phenomena is not considered in these references.

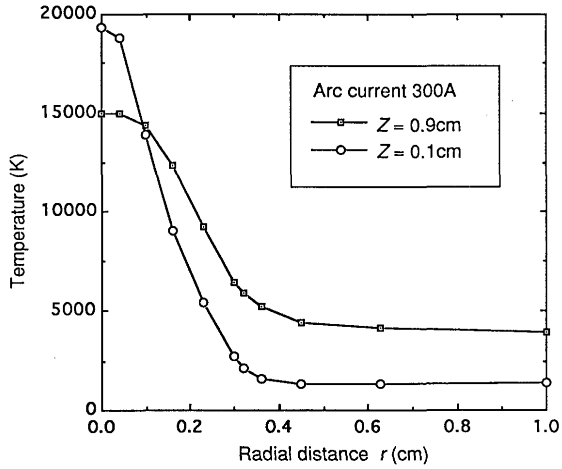


**Fig.5** Computed arc temperature distributions in the radial direction at sections near cathode and anode

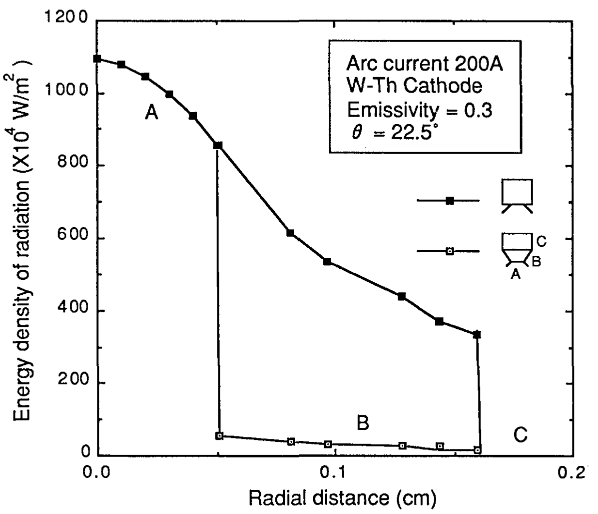


**Fig.6** Distribution of calculated radiation energy density on the conic-flat and flat cathode tips at 200A current.

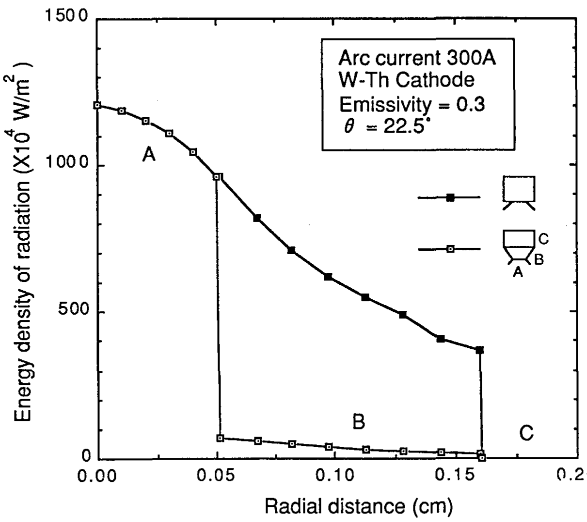


**Fig.7** Distribution of calculated radiation energy density on the conic-flat and flat cathode tips at 300A current.

In this calculation, the anode is taken to be a copper plate and the absorptivity at high temperature is about 0.2 [28]. According to Ref.4 and Ref.27 the absorptivity of Th-W electrode at high temperature is about 0.3. Though the calculation in this paper is limited to the special conditions, the contribution of radiation energy to rod electrodes or plates which have different emissivities may also be easily obtained by simply multiplying a factor of the emissivity ratio to the results of the present calculation.

## 3. Results and Discussion

### 3.1 Distribution of plasma radiation energy on the cathode

**Figure 6** shows the results of radiation energy density distribution absorbed by the cathode electrode for 200A current. We can see that for the electrode with a flat tip the absorbed radiation energy is approximately the Gauss distribution, i.e., the energy density at axial center is about 3 times higher than the side boundary. While when the tip of electrode is a frustum of a cone, as compared to the flat part(A), in the conical surface (B) the energy density suddenly decreases due to change of the incident angle. **Figure 7** shows the results for 300A arc current. The energy distribution is similar to 200A arc current, but there is some 10% increase in the magnitude. It is found that even for 300A arc current, the absorbed energy is almost zero on the side surface of the rod electrode. **Figure 8** represents the results for a pure cone type of electrode tip. As we see, the absorbed energy density is much less than the electrodes mentioned previously.

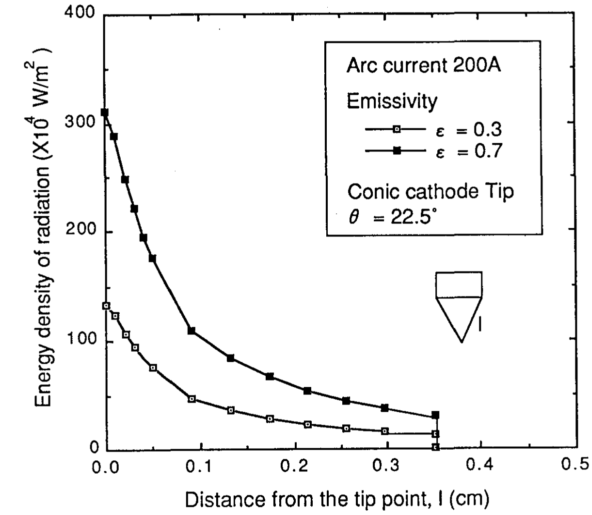


**Fig.8** Distribution of calculated radiation energy density on the conic cathode tip at 200A current.

### 3.2 Distribution of plasma radiation energy on the anode plate

**Figure 9** and **Fig.10** show the calculated results of plasma radiation energy density distribution on the copper anode plate for 200A and 300A, respectively. It is seen that a higher magnitude of distribution is displayed for a larger arc current, but it is lower than that on the cathode with a flat tip. This is because the arc temperature has a peak distribution in the near cathode zone (see Fig.4). Ref.26 also represented the radiation energy distribution on the anode plate for 200A arc current. It is found their result agrees very well with the results of present study.

In order to analyze the effects of arc length on the radiation energy distribution on the electrode or weldment, the contribution of radiation energy is

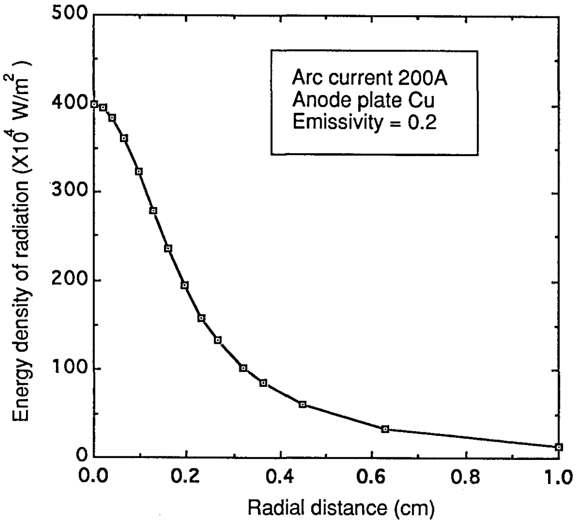


**Fig.9** Distribution of calculated radiation energy density on the anode plate at 200A current

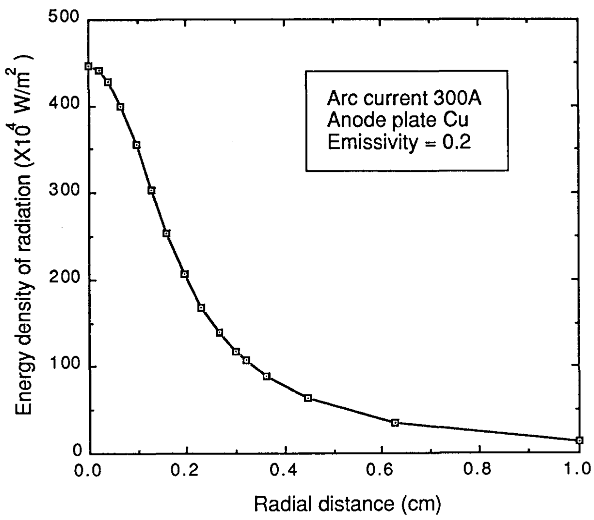


**Fig.10** Distribution of calculated radiation energy density on the anode plate at 300A current

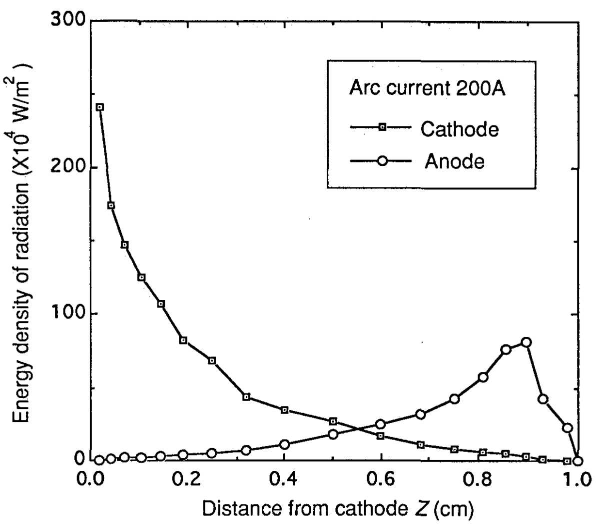


**Fig.11** Contribution of arc radiation energy to the axial center point of cathode and anode by various arc cross-section-elements at 200A current.

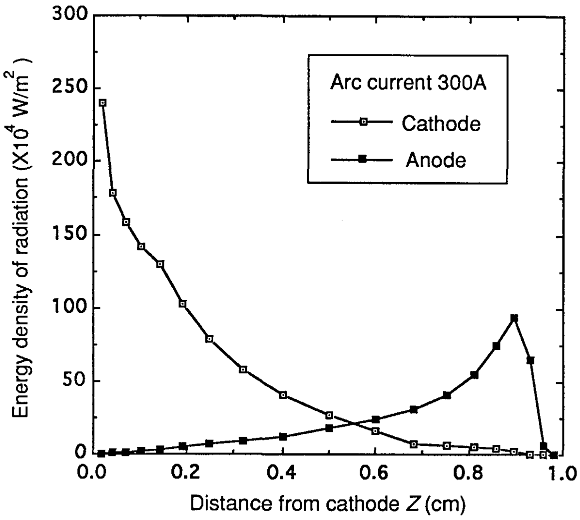


**Fig.12** Contribution of arc radiation energy to the axial center point of cathode and anode by various arc cross-section-elements at 300A current.

calculated to the axial center point of cathode and anode by various arc cross section elements, and the results are shown in **Fig.11** and **Fig.12**. It is found that about 90% energy comes from the plasma zone located near the electrodes, within 3mm for rod cathode and 4mm for anode plate. This implies that if the arc length is longer than 4mm, the excessive part contributes negligible radiation energy to the electrodes.

### 3.3 Total amount of radiation energy absorbed by the electrodes

The total radiation energy absorbed by the rod cathode and anode plate is obtained by integrating the energy distribution represented above, and the result is shown in **Fig.13**. We can see from this figure that the absorbed total radiation energy by the rod cathode is below 100W and by copper anode plate is not over 200W for the arc current up to 300A. The energy obtained by the cathode with a conical surface is only about half that of the flat tip. At the same condition (100A, cathode diameter 3.2mm, emissivity 0.3), the calculated radiation energy assimilated by the cathode in this study is only about 10% of that presented in Ref.4, and we think it must be over-estimated in Ref.4.

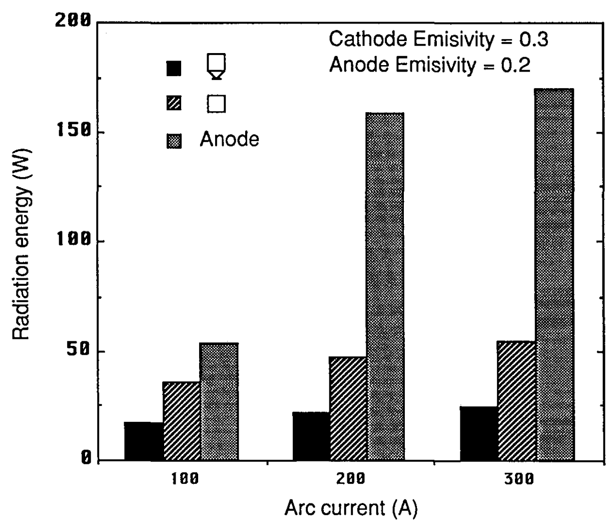


**Fig.13** Calculated total radiation energy absorbed by the rod cathode and plate anode at various current.

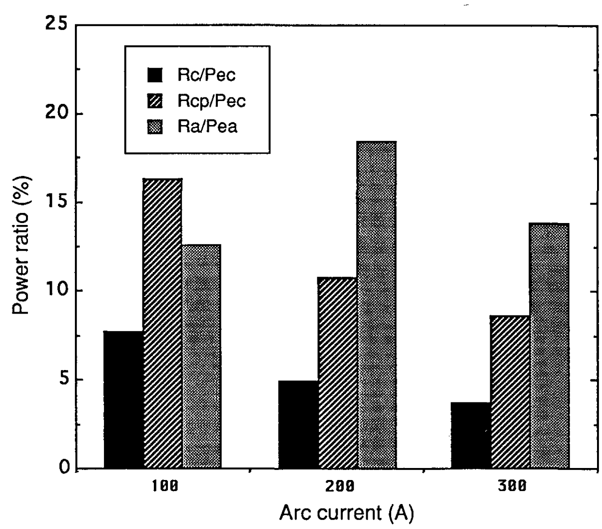


**Fig.14** Ratio of absorbed radiation energy to the electron energy for cathode and anode. $R_c$, $R_{cp}$, and $R_a$ represent the radiation energy of rod cathode with conic-flat and flat tip and anode plate, respectively. $P_{ec}$ and $P_{ea}$ represent the electron energy of cathode and anode, respectively.

### 3.4 Relative effect of radiation energy on the electrode energy balance

The relative effects of arc radiation energy on the cathode and anode energy balance can be evaluated by the ratio of radiation energy to the electron energy. Let's take the electron current on the cathode tip to be 85% of the total arc current $I$ [4,29], then the cathode electron cooling energy $P_{ec} \approx 0.85W_cI$, and the anode electron energy $P_{ea} \approx W_aI$, where the work function of cathode (W-Th) $W_c = 2.6$V, anode (Cu) $W_a = 4.3$V, thus the ratios are calculated and shown in **Fig.14**, where $R_c$, $R_{cp}$ and $R_a$ represent the radiation energy of rod cathode with conical-flat tip, flat tip and anode plate, respectively. It is found from Fig.14 that for the arc current varying from 100A to 300A, the relative contributions of plasma radiation energy to the electrodes are respectively about 8~17% for the flat electrode tip ($R_{cp}/P_{ec}$), 4~8% for the conic-flat electrode tip ($R_c/P_{ec}$), and 10~20% for the copper anode plate ($R_a/P_{ea}$). Another interesting finding from Fig.14 is that the relative contribution of plasma radiation energy to the cathode electrode decreases with increasing the arc current from 100A to 300A. This is because the electron cooling energy due to emission from the cathode surface is approximately proportional to the arc current, while the contribution of plasma radiation to the cathode is not so high.

## 4 Conclusion

(1) The contribution of arc radiation energy to the electrodes is small as compared to the electron cooling energy in cathode or heating energy in anode plate for Gas-Tungsten-Arcs with arc current from 100A to 300A. The arc radiation energy may, to some extent, have effects, especially in relatively lower current, but dose not play an dominant role in the cathode or anode energy balance.

(2) The radiation energy absorbed by the electrodes mainly comes from the arc plasma located in the near electrode zone, within about 3mm for rod cathode and 4mm for anode plate. This implies if the arc length is longer than 4mm, the excessive part contributes negligible radiation energy to the electrodes. The shape and size of rod electrode tip has a big effect on the total amount and distribution of absorbed radiation energy.

### References


1) M. Ushio, A.A. Sadek and F. Matsuda : Plasma Chem. & Plasma Processing, Vol.11 (1991), 81
2) J.Hackmann and H. Bebber : Pure & Appl. Chem., Vol.64 (1992), No.5, 353
3) J.F. Lancaster : The Physics of Welding, Pergamon Press (1986)
4) L.E. Cram : J. Phys. D Appl. Phys., Vol.16 (1983), 1643
5) J.F. Lancaster : British Weld. J., Vol.1 (1954), 412
6) G. Busz-Peuckert and W. Finkelnburg : J. Phys., Vol.144 (1956), 244
7) P.A. Schoeck : Ph. D. thesis, University of Minnesota (1961)
8) K. Ando and J. Nishikawa : IIW Document, 212-158-68 (1968)
9) N.A. Sanders and E. Pfender : J. Appl. Phys. Vol.55 (1984), 714
10) M. Ushio, D. Fan and M. Tanaka : A method of estimating the space-charge voltage drop for thermionic arc cathodes, The 6th of Symposium on Plasma Science for Materials (1993), 231
11) M. Ushio and F. Matsuda : IIW Document, 212-528-82 (1982).
12) D.L. Evans and R. S. Tankin : Phys. Fluids, Vol.10 (1967), 1137
13) H.W. Emmons : Phys. Fluids, Vol.10 (1967), 1125
14) P. Kovitya and J.J. Lowke : J. Phys. D Appl. Phys., Vol.18 (1985), 1125
15) R.G. Eckert and J. Goldstein : Measurements in heat transfer, Hemispgere publishing corporation (1976)
16) L.E. Cram : J. Phys. D Appl. Phys., Vol.18 (1985), 401
17) H.N. Olsen : Phys. Fluids, Vol.2 (1959), 614
18) A.E.F. Gick, M.B.C. Quigley and P.H. Richards : J. Phys. D Appl. Phys., Vol.6 (1973), 194
19) G. Seeger and W. Tiller : Arc physics and weld pool behaviour, Proc. Int. Con. Lond (1979), 25
20) M. Kobayashi and T. Suga : Arc physics and weld pool behaviour, Proc. Int. Con. Lond(1979), 315
21) J.F. Key, J.W. Chen and M.E. Mcllwain : Weld. J., Vol.62 (1983), 179s
22) G.N. Haddad and A.J.D. Farmer : J. Phys. D Appl. Phys., Vol.16 (1984), 1184
23) G.N. Haddad and A.J.D. Farmer : Weld. J., Vol.64 (1985), No.9, 226s
24) A.J.D. Farmer and G. N. Haddad : Appl. Phys. Lett., Vol.45 (1984), No.1, 25
25) K.C. Hsu, K. Etemadi and E. Pfender : J. Appl. Phys., Vol.54 (1983), 1293
26) R.T.C. Choo, J. Szekely and R.C. Westhoff : Welding Journal, No.9 (1990), 346
27) A.A. Sadek : Development of new tungsten electrode by rare earth metal oxide additions for inert gas DC arc welding, Ph.D. thesis of Osaka University (1989)
28) T. Ohji : J. Japan Weld. Soci., Vol.61 (1992), No.2, 92 (in Japanese)
29) K.C. Hsu and E. Pfender : J. Appl. Phys., Vol.74 (1993), 3818